IEEE Access
Multidisciplinary ⋮ Rapid Review ⋮ Open Access Journal

Received February 16, 2020, accepted February 29, 2020, date of publication March 11, 2020, date of current version March 20, 2020.

Digital Object Identifier 10.1109/ACCESS.2020.2980167

Performance Analysis and Fairness Maximization in NOMA Systems With Improper Gaussian Signaling Under Imperfect Successive Interference Cancellation

SEUNG GEUN HONG AND SAEWOONG BAHK, (Senior Member, IEEE)
Department of Electrical and Computer Engineering, INMC, Seoul National University, Seoul 08826, South Korea

Corresponding author: Saewoong Bahk (sbahk@snu.ac.kr)

This work was supported by the Institute of Information and Communications Technology Planning and Evaluation (IITP) grant funded by the Korea government (MSIT), Scalable Spectrum Sharing for Beyond 5G Communication, under Grant 2018-0-00923.

ABSTRACT In this paper, we investigate a downlink non-orthogonal multiple access (NOMA) system consisting of a base station (BS) and two users, where each user decodes its own signal through successive interference cancellation (SIC). When the signal of one user, called the weak user (WU) who has a bad channel, is being decoded, the signal of the other user, called the strong user (SU) who has a good channel, acts as interference. In an interference channel, we can increase the achievable rate by applying improper Gaussian signaling (IGS). Therefore, we apply IGS to SU, aiming to mitigate the interference. We also consider imperfect SIC at SU, which is a more general assumption for a NOMA system. For the considered NOMA system model, we derive the outage probability of each user in a closed form, provide its asymptotic expression, and obtain its diversity order. We also derive the ergodic rate of each of the two users in a closed form. We propose two algorithms to maximize the fairness of the NOMA system based on the primal decomposition method. Through simulation, we verify that our analysis is correct, and confirm that applying IGS improves the fairness of the NOMA system.

INDEX TERMS Ergodic rate, fairness, imperfect successive interference cancellation (SIC), improper Gaussian signaling (IGS), non-orthogonal multiple access (NOMA) system, outage probability, primal decomposition.

I. INTRODUCTION

Non-orthogonal multiple access (NOMA) is a promising technology to improve spectral efficiency of future wireless communication systems [1]–[5]. The power domain multiplexing is the main idea of NOMA such that the base station (BS) broadcasts the superposed signals for multiple users with different powers, and each receiver decodes its own signal through the successive interference cancellation (SIC) technique. Compared with a conventional orthogonal multiple access (OMA) scheme where one channel is assigned to only one user, a NOMA scheme allows multiple users to use the same channel to achieve higher rates and lower outage probabilities.

The associate editor coordinating the review of this manuscript and approving it for publication was Jie Tang.

In a two-user downlink NOMA system, the BS allocates more power to a user whose channel condition has been significantly degraded due to path loss and shadowing effects, called the weak user (WU), than the other user, called the strong user (SU) who has a better channel [1]–[3], [6]. WU decodes its own signal by treating SU's signal as interference. SU performs SIC, i.e., it decodes WU's signal first and cancels it from the received signal. After SIC, SU decodes its own signal. Since SU's signal acts as interference while WU decodes its signal and SU performs SIC, it should be mitigated to improve the performance of the NOMA system.

Proper Gaussian signaling (PGS) is a common assumption in communication systems, where a signal is assumed to be circularly symmetric complex Gaussian distributed, i.e., its real and imaginary parts have equal power and they are independently zero-mean Gaussian distributed [7], [8].

By the maximum entropy theorem, PGS is known to achieve the maximum achievable rate in an additive white Gaussian noise (AWGN) channel [7]. Due to this, most studies on communication systems assume PGS. However, PGS may not be an optimal choice in an interference channel.

In [9]–[11], the authors show that improper Gaussian signaling (IGS) can improve the achievable rate over PGS in an interference channel. Compared to PGS, IGS is a more general class of signals where circularity and uncorrelatedness conditions are relaxed. This means, real and imaginary parts of a signal either have unequal power or are correlated [7], [8]. In practical digital communication systems, binary phase shift keying (BPSK) and continuous phase modulation (CPM) are the well known improper signal modulation schemes [12], and more general improper signal modulation schemes are investigated in [13].

There has been a lot of research on the adoption of IGS to improve the performance for various interference channel scenarios. In [14]–[16], the performance is improved by using IGS in the Z-interference channel. In [17] and [18], a secondary user with IGS achieves higher rate by avoiding interference from a primary user. In [19], IGS improves the achievable rate of an alternate relaying system by reducing inter-relay interference. In [20], IGS improves both the outage probability and the ergodic capacity in a full-duplex relaying system by reducing residual self interference.

By applying IGS to NOMA, interference of SU's signal can be reduced, which improves the performance of NOMA systems. There are several studies on NOMA systems with IGS [21], [22]. In [21], the authors maximize instantaneous sum rate by controlling impropriety of signals in a two-user NOMA system. In [22], it shows that transmit beamforming contributes to maximizing the minimum throughput of users in a multiuser multi-cell NOMA system with IGS. These works are based on the assumption of using instantaneous channel state information (CSI) where the BS knows perfect CSI of each user. However, due to limited resources for uplink feedback, instantaneous CSI may not be available at the BS. In this scenario, we should consider statistical CSI, which can be obtained easily according to the location of each user.

When analyzing the performance of a communication system with statistical CSI, the most commonly used metrics are the outage probability and ergodic capacity. In a slow fading channel, an outage occurs when a user suffers deep fading, resulting in unreliable communication at a certain rate [23]. In contrast, in a fast fading channel, a user may avoid an outage because it does not suffer deep fading, so that reliable communication at a certain rate is possible [23]. Therefore, the outage probability and ergodic capacity are commonly used in the former and latter scenarios, respectively.

Most of the existing work on NOMA systems assumes perfect SIC at the receiver, i.e., SU cancels WU's signal from the received signal perfectly. This is not practical due to various reasons such as synchronization error, channel estimation error, and imperfect decoding [24], [34]. Therefore, considering imperfect SIC at the receiver is a viable approach for NOMA systems.

In this paper, we investigate a downlink NOMA system consisting of a BS and two users, where SIC at SU is not perfect. SU uses IGS while WU uses PGS. Our approach improves the performance of WU while sacrificing that of SU, i.e., a compromise to improve fairness between the two users. The contributions of this paper are as follows:

- We consider a NOMA system where statistical CSI is available at the BS. Assuming imperfect SIC at SU, we derive the outage probability of each user in a closed form and reveal the impact of imperfect SIC on performance. We also derive the asymptotic expression, diversity order, ergodic rate of each user.
- We formulate the fairness optimization problem and use two-dimensional grid search to get its optimal solution. To reduce the computational complexity, we propose an algorithm that uses the primal decomposition method.
- Through simulation, we confirm that our analysis is accurate, and show that the proposed algorithms achieve much better performance than two-dimensional grid search in terms of runtime. We also show that applying IGS improves fairness of the NOMA system.

The remainder of this paper is organized as follows. In Section II, we describe the model of the NOMA system with IGS under imperfect SIC. In Section III, we derive the outage probability, diversity order, and ergodic rate of each user. In Section IV, we propose algorithms to maximize the fairness of the NOMA system. Section V presents Monte Carlo simulation results, followed by the conclusions in Section VI.

II. SYSTEM MODEL

We consider a downlink NOMA system that consists of a BS and two users, i.e., WU and SU. WU is a user whose channel condition has been significantly degraded due to path loss and shadowing effects, and SU is the other user. Each user has a single antenna.

A. CHANNEL MODEL

Suppose that the BS has only statistical CSI, not instantaneous CSI. This means, the BS does not know the exact channel coefficients, but it knows the channel variance.

Assume that the channel coefficients from the BS to WU and SU, h_w and h_s, are independent zero mean complex Gaussian random variables with variance λ_w and λ_s, respectively. Note that $\lambda_w < \lambda_s$.

We denote the channel gains of WU and SU by $g_w = |h_w|^2$ and $g_s = |h_s|^2$, respectively. The probability density functions (pdfs) of channel gains g_w and g_s are given by

$$f_{g_w}(g) = \frac{1}{\lambda_w} e^{-\frac{1}{\lambda_w} g}, \tag{1}$$

and

$$f_{g_s}(g) = \frac{1}{\lambda_s} e^{-\frac{1}{\lambda_s} g}, \tag{2}$$

respectively.

B. RECEIVED SIGNAL MODEL

The transmit signal at the BS intended for WU and SU are denoted by x_w and x_s, respectively. Let $\alpha \in (0, 0.5)$ denote the power allocation factor for SU's signal. The BS sends the superposed signal, i.e., $\sqrt{1-\alpha}x_w + \sqrt{\alpha}x_s$, with transmit power P. The received signal at WU is given by

$$y_w = \sqrt{P}(\sqrt{1-\alpha}x_w + \sqrt{\alpha}x_s)h_w + n_w \tag{3}$$

where n_w is the AWGN at WU with variance $\sigma^2_{n_w}$. The received signal at SU is given by

$$y_s = \sqrt{P}(\sqrt{\alpha}x_s + \sqrt{1-\alpha}x_w)h_s + n_s \tag{4}$$

where n_s is the AWGN at SU with variance $\sigma^2_{n_s}$. Assume that the noise variances at the both users are the same and normalized, i.e., $\sigma^2_{n_s} = \sigma^2_{n_w} = \sigma^2 = 1$. Suppose that SU performs SIC, i.e., SU decodes WU's signal and cancels it from the received signal [1], [2]. After SIC, the received signal of SU becomes

$$y_s = \sqrt{P\alpha}x_s h_s + \sqrt{P(1-\alpha)}x_w h_r + n_s \tag{5}$$

where h_r represents the residual interference channel coefficient for imperfect SIC at SU. We use the imperfect decoding model for imperfect SIC where the residual interference is modeled as complex Gaussian random variable [25]–[29].[1] Assume that h_r is a complex Gaussian random variable with zero mean and variance $\xi\lambda_s$, where ξ represents the level of residual interference. So the cases of $\xi = 0$ and 1 indicate perfect SIC and fully imperfect SIC, respectively.[2]

C. IMPROPER GAUSSIAN SIGNALING

IGS shows its advantages when treated as interference [11]. Since the two users decode WU's signal by treating SU's signal as interference, we apply IGS to SU to mitigate the effects of interference, and then PGS to WU.[3] The impropriety of signal x is defined as follows:

Definition 1 [7], [8]: The variance and pseudo variance of signal x are given by $\sigma_x^2 = \mathbb{E}[|x|^2]$ and $\tilde{\sigma}_x^2 = \mathbb{E}[x^2]$, respectively.

Definition 2 [7], [8]: If $\tilde{\sigma}_x^2 = 0$, signal x is called proper, otherwise improper.

Definition 3 [17]: A circularity coefficient of signal x is given by $\mathcal{C}_x = |\tilde{\sigma}_x^2|/\sigma_x^2$.

From the definitions, the circularity coefficient of signal x satisfies $\mathcal{C}_x \in [0, 1]$. The cases of $\mathcal{C}_x = 0$ and 1 indicate the proper and maximally improper signals, respectively.

[1]In practical digital communication systems, signals are not Gaussian distributed. In these cases, residual interference may not be modeled as a Gaussian random variable as in [30]–[33]. These cases are beyond our scope, but should be considered in future work dealing with practical scenarios.

[2]The residual interference from imperfect decoding should be modeled as $h_s e_r$ where $e_r \sim \mathcal{CN}(0, \xi)$ represents the error resulted from imperfect decoding [34]. However, because this model makes the analysis too complicated, we simplify residual interference to $h_r \sim \mathcal{CN}(0, \xi\lambda_s)$ instead of $h_s e_r$, which is a widely used model as in [25]–[29].

[3]By applying IGS to WU may improve the performance of the NOMA system because WU's signal is also treated as interference in (5). However, this makes the analysis too complicated and is beyond our scope, so that we leave this as future work.

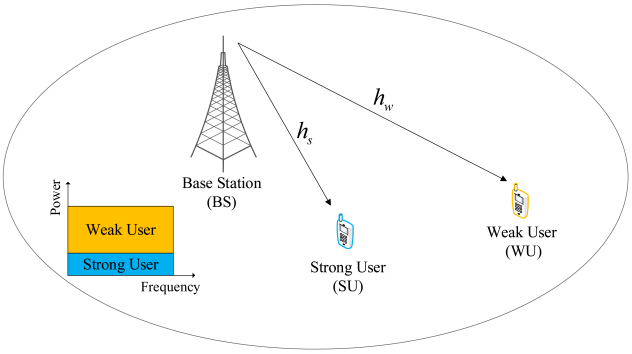

FIGURE 1. System model of the two-user downlink NOMA system.

D. ACHIEVABLE RATES

When IGS is applied, for a received signal y and an interference-plus-noise signal z, the achievable rate is given by [11]

$$R = \frac{1}{2}\log_2\left(\frac{\sigma_y^4 - |\tilde{\sigma}_y^2|^2}{\sigma_z^4 - |\tilde{\sigma}_z^2|^2}\right). \tag{6}$$

From (3) and (6), we obtain the achievable rate of WU as

$$R_w = \frac{1}{2}\log_2\left(\frac{(Pg_w+1)^2 - (P\alpha g_w \mathcal{C}_{x_s})^2}{(P\alpha g_w+1)^2 - (P\alpha g_w \mathcal{C}_{x_s})^2}\right). \tag{7}$$

From (4) and (6), we can obtain the achievable rate of SU for decoding WU's signal, as

$$R_{s\to w} = \frac{1}{2}\log_2\left(\frac{(Pg_s+1)^2 - (P\alpha g_s \mathcal{C}_{x_s})^2}{(P\alpha g_s+1)^2 - (P\alpha g_s \mathcal{C}_{x_s})^2}\right). \tag{8}$$

From (5) and (6), we have the achievable rate of SU after SIC as

$$R_{s\to s} = \frac{1}{2}\log_2\left(\frac{(P\alpha g_s + P(1-\alpha)g_r+1)^2 - (P\alpha g_s \mathcal{C}_{x_s})^2}{(P(1-\alpha)g_r+1)^2}\right) \tag{9}$$

where $g_r = |h_r|^2$ is the gain of the residual interference channel.

III. PERFORMANCE ANALYSIS

A. OUTAGE PROBABILITY OF WU

When the achievable rate of WU is lower than the target rate $R_{t,w}$, an outage occurs. The outage probability of WU is given by

$$p_w^{\text{out}} = \Pr[R_w < R_{t,w}]. \tag{10}$$

Putting (7) into (10), we get

$$p_w^{\text{out}} = \Pr[\underbrace{P^2(1-\alpha^2\gamma_w + \alpha^2\gamma_w\mathcal{C}_{x_s}^2 - \alpha^2\mathcal{C}_{x_s}^2)}_{=A} g_w^2 + \underbrace{2P(1-\alpha\gamma_w)}_{=B} g_w - (\gamma_w - 1) < 0] \tag{11}$$

where $\gamma_w = 2^{2R_{t,w}}$ ($\gamma_w > 1$ since $R_{t,w} > 0$). The following lemma shows the available range of the power allocation factor α and the circularity coefficient of SU's signal $\mathcal{C}_{x_s}$.

Lemma 1: For the outage probability of WU not to be one, the following inequality should hold:

$$\alpha < \frac{1}{\sqrt{1+(\gamma_w-1)(1-\mathcal{C}_{x_s}^2)}}. \tag{12}$$

Proof: The proof is given in Appendix A. ■

In the rest of this paper, we only consider the case when Eq. (12) holds. We can see that, in the quadratic function inside the probability in (11), the second order coefficient of g_w is positive and the y-intercept is negative. So the quadratic function has only one positive root, which is given by

$$g_w^0 = \frac{-(1-\alpha\gamma_w)+\sqrt{\gamma_w(1-\alpha)^2+(\gamma_w-1)^2\alpha^2\mathcal{C}_{x_s}^2}}{P(1-\alpha^2(1+(\gamma_w-1)(1-\mathcal{C}_{x_s}^2)))}. \tag{13}$$

The inequality inside the probability in (11) holds when g_w is smaller than the positive root, i.e., $g_w \in (0, g_w^0)$. Using this, we derive the outage probability of WU in the following theorem.

Theorem 1: The outage probability of WU is given by

$$p_w^{\text{out}} = 1 - e^{-\frac{1}{\lambda_w}g_w^0}. \tag{14}$$

Proof: Since the outage occurs at WU when $g_w \in (0, g_w^0)$, we can obtain the outage probability of WU by integrating the pdf of g_w over the region $g_w \in (0, g_w^0)$, i.e.,

$$p_w^{\text{out}} = \int_0^{g_w^0} f_{g_w}(g)dg \tag{15}$$

which gives the result of the theorem. ■

B. OUTAGE PROBABILITY OF SU

When SU's achievable rate for decoding the signal of WU is lower than the target rate $R_{t,w}$ or that of SU is lower than the target rate $R_{t,s}$, an outage occurs. Thus we can express the outage probability of SU as

$$\begin{aligned} p_s^{\text{out}} &= \Pr[R_{s\to w} < R_{t,w} \cup R_{s\to s} < R_{t,s}] \\ &= \underbrace{\Pr[R_{s\to w} < R_{t,w}]}_{=C} + \underbrace{\Pr[R_{s\to s} < R_{t,s} \cap R_{s\to w} > R_{t,w}]}_{=D}. \end{aligned} \tag{16}$$

Using the fact that the formulas of $R_{s\to w}$ and R_w are similar to each other, $R_{s\to w} < R_{t,w}$ holds for $g_s \in (0, g_w^0)$. Therefore, the outage probability of SU for decoding WU's signal is given by

$$\begin{aligned} C &= \Pr[R_{s\to w} < R_{t,w}] \\ &= \int_0^{g_w^0} f_{g_s}(g)dg \\ &= 1 - e^{-\frac{1}{\lambda_s}g_w^0}. \end{aligned} \tag{17}$$

Since $R_{s\to w} > R_{t,w}$ holds for $g_s \in (g_w^0, \infty)$, we obtain the second term on the right hand side (RHS) of (16) as

$$\begin{aligned} D &= \Pr[R_{s\to s} < R_{t,s} \cap R_{s\to w} > R_{t,w}] \\ &= \int_{g_w^0}^{\infty} \underbrace{\Pr[R_{s\to s} < R_{t,s} | g_s = g]}_{=E} f_{g_s}(g)dg. \end{aligned} \tag{18}$$

Putting (9) into (18), we have the conditional probability in the integration on the RHS of (18) as

$$\begin{aligned} E &= \Pr[R_{s\to s} < R_{t,s} | g_s = g] \\ &= \Pr[P^2(\gamma_s-1)(1-\alpha)^2 g_r^2 - 2P(1-\alpha)(P\alpha g_s - (\gamma_s-1))g_r \\ &\quad -P^2\alpha^2(1-\mathcal{C}_{x_s}^2)g_s^2 - 2P\alpha g_s + (\gamma_s-1) > 0 | g_s = g] \end{aligned} \tag{19}$$

where $\gamma_s = 2^{2R_{t,s}}$. The following lemma shows the range of g_r where an outage at SU occurs.

Lemma 2: For $g_s \in (0, g_s^0)$, the inequality $R_{s\to s} < R_{t,s}$ always holds regardless of g_r, where

$$g_s^0 = \frac{-1+\sqrt{1+(\gamma_s-1)(1-\mathcal{C}_{x_s}^2)}}{P\alpha(1-\mathcal{C}_{x_s}^2)}. \tag{20}$$

For $g_s \in (g_s^0, \infty)$, the inequality $R_{s\to s} < R_{t,s}$ holds if and only if $g_r \in (g_r^0(g_s), \infty)$, where

$$g_r^0(g_s) = \frac{P\alpha\left(1+\sqrt{1+(\gamma_s-1)(1-\mathcal{C}_{x_s}^2)}\right)g_s - (\gamma_s-1)}{P(\gamma_s-1)(1-\alpha)}. \tag{21}$$

Proof: The proof is given in Appendix B. ■

From Lemma 2, we obtain the conditional probability in (19) as

$$\begin{aligned} E &= \Pr[R_{s\to s} < R_{t,s} | g_s = g] \\ &= \begin{cases} 1, & g \in (0, g_s^0), \\ \int_{g_r^0(g)}^{\infty} f_{g_r}(\tilde{g})d\tilde{g}, & g \in (g_s^0, \infty), \end{cases} \\ &= \begin{cases} 1, & g \in (0, g_s^0), \\ e^{-\frac{1}{\xi\lambda_s}g_r^0(g)}, & g \in (g_s^0, \infty). \end{cases} \end{aligned} \tag{22}$$

Putting (22) into (18), we derive the second term on the RHS of (16) as

$$\begin{aligned} D &= \int_{g_w^0}^{\infty} E f_{g_s}(g)dg \\ &= \begin{cases} \int_{g_w^0}^{g_s^0} f_{g_s}(g)dg + \int_{g_s^0}^{\infty} e^{-\frac{1}{\xi\lambda_s}g_r^0(g)} f_{g_s}(g)dg, & g_w^0 < g_s^0, \\ \int_{g_w^0}^{\infty} e^{-\frac{1}{\xi\lambda_s}g_r^0(g)} f_{g_s}(g)dg, & g_w^0 > g_s^0, \end{cases} \\ &= \begin{cases} e^{-\frac{1}{\lambda_s}g_w^0} - e^{-\frac{1}{\lambda_s}g_s^0} + \Xi e^{-\frac{1}{\xi\lambda_s}g_r^0(g_s^0)} e^{-\frac{1}{\lambda_s}g_s^0}, & g_w^0 < g_s^0, \\ \Xi e^{-\frac{1}{\xi\lambda_s}g_r^0(g_w^0)} e^{-\frac{1}{\lambda_s}g_w^0}, & g_w^0 > g_s^0, \end{cases} \end{aligned} \tag{23}$$

where

$$\Xi = \frac{(\gamma_s-1)(1-\alpha)\xi}{\alpha\left(1+\sqrt{1+(\gamma_s-1)(1-\mathcal{C}_{x_s}^2)}\right)+(\gamma_s-1)(1-\alpha)\xi}. \tag{24}$$

Finally, we derive the outage probability of SU in the following theorem.

Theorem 2: The outage probability of SU is given by

$$p_s^{\text{out}} = 1 - e^{-\frac{1}{\lambda_s}g_{\max}}(1 - \Xi e^{-\frac{1}{\xi\lambda_s}g_r^0(g_{\max})}) \tag{25}$$

where $g_{\max} = \max(g_w^0, g_s^0)$.

Proof: Putting (17) and (23) into (16), we obtain the outage probability of SU as

$$p_s^{\text{out}} = C + D = \begin{cases} 1 - e^{-\frac{1}{\lambda_s} g_s^0} + \Xi e^{-\frac{1}{\xi\lambda_s} g_r^0(g_s^0)} e^{-\frac{1}{\lambda_s} g_s^0}, & g_w^0 < g_s^0, \\ 1 - e^{-\frac{1}{\lambda_s} g_w^0} + \Xi e^{-\frac{1}{\xi\lambda_s} g_r^0(g_w^0)} e^{-\frac{1}{\lambda_s} g_w^0}, & g_w^0 > g_s^0, \end{cases} \tag{26}$$

which gives the result of the theorem. ■

Corollary 1: The outage probability of SU with perfect SIC is given by

$$p_s^{\text{out-perfect}} = 1 - e^{-\frac{1}{\lambda_s} g_{\max}}. \tag{27}$$

Proof: If SIC is perfect, i.e., $\xi \to 0$, then $\Xi \to 0$ which gives the result of the corollary. ■

Comparing (25) and (27), we can see that the term $\Xi e^{-\frac{1}{\xi\lambda_s} g_r^0(g_{\max})}$ in p_s^{out} comes from imperfect SIC.

C. OUTAGE PROBABILITY IN HIGH SNR

As $P \to \infty$, the values of g_w^0, g_s^0, $g_{\max}$, and $g_r^0(g_{\max})$ converge to

$$\begin{aligned} &\lim_{P\to\infty} g_w^0 \\ &= \lim_{P\to\infty} \frac{-(1-\alpha\gamma_w) + \sqrt{\gamma_w(1-\alpha)^2 + (\gamma_w-1)^2\alpha^2\mathcal{C}_{x_s}^2}}{P(1-\alpha^2(1+(\gamma_w-1)(1-\mathcal{C}_{x_s}^2)))} \\ &= 0, \end{aligned} \tag{28}$$

$$\begin{aligned} &\lim_{P\to\infty} g_s^0 \\ &= \lim_{P\to\infty} \frac{-1 + \sqrt{1+(\gamma_s-1)(1-\mathcal{C}_{x_s}^2)}}{P\alpha(1-\mathcal{C}_{x_s}^2)} \\ &= 0, \end{aligned} \tag{29}$$

$$\begin{aligned} &\lim_{P\to\infty} g_{\max} \\ &= \max\left(\lim_{P\to\infty} g_w^0, \lim_{P\to\infty} g_s^0\right) \\ &= 0, \end{aligned} \tag{30}$$

and

$$\begin{aligned} &\lim_{P\to\infty} g_r^0(g_{\max}) \\ &= \lim_{P\to\infty} \frac{P\alpha\left(1+\sqrt{1+(\gamma_s-1)(1-\mathcal{C}_{x_s}^2)}\right) g_{\max} - (\gamma_s-1)}{P(\gamma_s-1)(1-\alpha)} \\ &= \lim_{P\to\infty} \left[\frac{\alpha\left(1+\sqrt{1+(\gamma_s-1)(1-\mathcal{C}_{x_s}^2)}\right)}{(\gamma_s-1)(1-\alpha)} g_{\max} - \frac{1}{P(1-\alpha)}\right] \\ &= 0, \end{aligned} \tag{31}$$

respectively. Then, we can obtain the asymptotic expression of the outage probability for each user in the following corollary.

Corollary 2: The outage probability of WU in the high SNR is approximated as

$$p_w^{\text{out}} \approx \frac{1}{\lambda_w} g_w^0. \tag{32}$$

The outage probabilities of SU with perfect SIC and imperfect SIC in the high SNR are approximated as

$$p_s^{\text{out-perfect}} \approx \frac{1}{\lambda_s} g_{\max}. \tag{33}$$

and

$$p_s^{\text{out}} \approx \Xi, \tag{34}$$

respectively.

Proof: Using the approximation $1 - e^{-x} \approx x$ for $x \to 0$, we can easily obtain (32) and (33) from (14) and (27), respectively. For the imperfect SIC case, it is easy to see that the outage probability of SU with imperfect SIC does not converges to zero. If $P \to \infty$ in (25), we can obtain (34). ■

It is easy to see that g_w^0 and g_s^0 are proportional to P^{-1}, and $g_{\max}$ is also proportional to P^{-1}. Therefore, from the definition of the diversity order $D = -\lim_{P\to\infty} \log(p^{\text{out}})/\log(P)$ and Corollary 2, we can see that WU and SU with perfect SIC achieve diversity order one. However, the imperfect SIC causes zero diversity order for SU.

D. ERGODIC RATES OF WU AND SU

We denote the ergodic rates of WU and SU as

$$\bar{R}_w = \mathbb{E}[R_w] \tag{35}$$

and

$$\bar{R}_s = \mathbb{E}[R_{s\to s}], \tag{36}$$

respectively. We present the closed-form expressions for the ergodic rates of WU and SU in the following theorem.

Theorem 3: The ergodic rate of WU is given by

$$\bar{R}_w = \frac{1}{2\ln 2}(-\Psi(\lambda_w, \alpha\mathcal{C}_{x_s}) + \Psi(\alpha\lambda_w, \mathcal{C}_{x_s})) \tag{37}$$

where

$$\begin{aligned} &\Psi(z, C) \\ &= e^{\frac{1}{Pz(1-C)}} \text{Ei}\left(-\frac{1}{Pz(1-C)}\right) + e^{\frac{1}{Pz(1+C)}} \text{Ei}\left(-\frac{1}{Pz(1+C)}\right), \end{aligned} \tag{38}$$

where $\text{Ei}(z) = -\int_{-z}^{\infty} \frac{e^{-t}}{t} dt$.

The ergodic rate of SU is given by

$$\bar{R}_s = -\frac{1}{2\ln 2}(\Omega(\mathcal{C}_{x_s}) + \Omega(-\mathcal{C}_{x_s})), \tag{39}$$

where

$$\begin{aligned} &\Omega(C) \\ &= \frac{\alpha(1-C)}{(1-\alpha)\xi - \alpha(1-C)} \left[e^{\frac{1}{P(1-\alpha)\xi\lambda_s}} \text{Ei}\left(-\frac{1}{P(1-\alpha)\xi\lambda_s}\right)\right. \\ &\quad \left. - e^{\frac{1}{P\alpha\lambda_s(1-C)}} \text{Ei}\left(-\frac{1}{P\alpha\lambda_s(1-C)}\right)\right]. \end{aligned} \tag{40}$$

Proof: The proof is given in Appendix C. ■

Corollary 3: The ergodic rate of SU with perfect SIC is given by

$$\bar{R}_s^{\text{perfect}} = -\frac{1}{2\ln 2}\Psi(\alpha\lambda_s, \mathcal{C}_{x_s}). \tag{41}$$

Proof: For $x > 0$, the following inequality holds [35]

$$\frac{1}{2}\ln\left(1+\frac{2}{x}\right) < -e^x \text{Ei}(-x) < \ln\left(1+\frac{1}{x}\right). \tag{42}$$

Since $\lim_{x\to\infty}\frac{1}{2}\ln\left(1+\frac{2}{x}\right) = 0$ and $\lim_{x\to\infty}\ln\left(1+\frac{1}{x}\right) = 0$, it is clear that $\lim_{x\to\infty} e^x\text{Ei}(-x) = 0$. Then we can easily obtain the ergodic rate of SU with perfect SIC from (39) by substituting ξ with 0. ■

IV. FAIRNESS OPTIMIZATION

A. PROBLEM FORMULATION

By adjusting the power allocation factor α and the circularity coefficient $\mathcal{C}_{x_s}$, we can improve the fairness of the NOMA system. If statistical CSI is available, fairness is maximized when the maximum outage probability of the two users is minimized [36]. We formulate the optimization problem to maximize the fairness of the NOMA system as

$$\begin{aligned}&\min_{\alpha,\mathcal{C}_{x_s}} \max(p_w^{\text{out}}, p_s^{\text{out}})\\ &\text{subject to}: 0 \le \mathcal{C}_{x_s} \le 1,\\ &\qquad 0 \le \alpha \le \min\left(\frac{1}{\sqrt{1+(\gamma_w-1)(1-\mathcal{C}_{x_s}^2)}}, 0.5\right),\end{aligned} \tag{43}$$

where the constraint of the power allocation factor comes from Lemma 1.

B. TWO-DIMENSIONAL GRID SEARCH

We use exhaustive search to obtain the optimal solution of the problem (43). Thanks to the closed form expressions for the outage probabilities of WU and SU, by using two-dimensional grid search, we can easily obtain the optimal solution that requires the computational complexity of $\mathcal{O}(1/\varepsilon^2)$, where ε is a search step size of two-dimensional grid search. The two-dimensional grid search method is briefly presented in Algorithm 1.

C. SUBOPTIMAL ALGORITHM BASED ON EXACT OUTAGE PROBABILITY

The objective function of the problem (43) has a closed form with elementary functions, but two-dimensional grid search may take a long time due to hardware limitations. To reduce the computational complexity, we propose an algorithm based on the primal decomposition method, which is widely used for solving resource allocation problems [37]–[39]. The considered problem is not convex, so its solution will be suboptimal without guaranteeing optimality. We will show the optimality and processing time of the proposed algorithm in Section V.

Algorithm 1 Two-Dimensional Grid Search

Initialize
  Set a search step size $\varepsilon > 0$ as a small positive number.
  Set $p^* = 1$.
for $\mathcal{C}_{x_s} = 0 : \varepsilon : 1$ **do**
  for $\alpha = 0 : \varepsilon : \min\left(\frac{1}{\sqrt{1+(\gamma_w-1)(1-\mathcal{C}_{x_s}^2)}}, 0.5\right)$ **do**
    Calculate $p_{\max} = \max(p_w^{\text{out}}, p_s^{\text{out}})$
    if $p_{\max} < p^*$ **then**
      $p^* = p_{\max}$ ▷ optimal outage probability
      $\mathcal{C}_{x_s}^* = \mathcal{C}_{x_s}$ ▷ optimal circularity coefficient
      $\alpha^* = \alpha$ ▷ optimal power allocation factor
    end if
  end for
end for

We divide the problem (43) into a master problem and a subproblem. The master problem determines the power allocation factor and the subproblem determines the circularity coefficient. For the fixed circularity coefficient $\mathcal{C}_{x_s}$, we formulate the master problem as

$$\begin{aligned}&\min_{\alpha} \max(p_w^{\text{out}}, p_s^{\text{out}})\\ &\text{subject to}: 0 \le \alpha \le \min\left(\frac{1}{\sqrt{1+(\gamma_w-1)(1-\mathcal{C}_{x_s}^2)}}, 0.5\right).\end{aligned} \tag{44}$$

Due to the non-convexity and complicated expression of the outage probability of each user, solving the problem (44) analytically is difficult. So, we find the optimal solution to the problem (44) with one-dimensional grid search.

For the fixed power allocation factor α, we formulate the subproblem as

$$\begin{aligned}&\min_{\mathcal{C}_{x_s}} \max(p_w^{\text{out}}, p_s^{\text{out}})\\ &\text{subject to}: \max\left(0, \frac{\alpha^2\gamma_w - 1}{\alpha^2(\gamma_w-1)}\right) \le \mathcal{C}_{x_s} \le 1\end{aligned} \tag{45}$$

where the constraint comes from the inequality $\alpha \le 1/\sqrt{1+(\gamma_w-1)(1-\mathcal{C}_{x_s}^2)}$. Similarly, we find the optimal solution to the problem (45) with one-dimensional grid search.

By solving the master problem and the subproblem iteratively, which is depicted in Algorithm 2, we can obtain the suboptimal solution to the problem (43). Algorithm 2 always converges since $\max(p_w^{\text{out}}, p_s^{\text{out}})$ always decreases in each iteration and $\max(p_w^{\text{out}}, p_s^{\text{out}}) > 0$. As one-dimensional grid search is used in each iteration, the computational complexity of Algorithm 2 is $\mathcal{O}(N/\varepsilon)$, where N is the number of iterations and ε is the search step size of one-dimensional grid search. For accuracy, ε is usually set to a very small positive number. Therefore, for $N \ll 1/\varepsilon$, our proposed algorithm has

Algorithm 2 Suboptimal Solution Based on Exact Analysis

Initialize
  Set a convergence parameter $\epsilon > 0$ as a small positive number.
  Set α and $\mathcal{C}_{x_s}$ satisfying the constraint of the problem (43).
  Set $p^* = \max(p_w^{\text{out}}, p_s^{\text{out}})$.
repeat
  For given $\mathcal{C}_{x_s}$, find α^* by solving the problem (44) with one-dimensional grid search.
  Set $\alpha = \alpha^*$.
  For given α, find $\mathcal{C}_{x_s}^*$ by solving the problem (45) with one-dimensional grid search.
  Set $\mathcal{C}_{x_s} = \mathcal{C}_{x_s}^*$.
  Set $p_{\text{prev}}^* = p^*$.
  Set $p^* = \max(p_w^{\text{out}}, p_s^{\text{out}})$.
until $p_{\text{prev}}^* - p^* < \epsilon$

much lower computational complexity than two-dimensional grid search.

D. SUBOPTIMAL ALGORITHM BASED ON ASYMPTOTIC OUTAGE PROBABILITY

Algorithm 2 uses one-dimensional grid search that still has high computational complexity. To reduce the complexity further, we propose an algorithm based on the asymptotic outage probability of each user and use the primal decomposition method. Before formulating a problem, we check the monotonic property of $g_w^0(\alpha, \mathcal{C}_{x_s})$ and $\Xi(\alpha, \mathcal{C}_{x_s})$.

The achievable rate of WU in (7) is strictly decreasing for α and strictly increasing for $\mathcal{C}_{x_s}$. This results in the outage probability of WU being strictly increasing for α and strictly decreasing for $\mathcal{C}_{x_s}$. Therefore, from (14), it is easy to see that $g_w^0(\alpha, \mathcal{C}_{x_s})$ is strictly increasing for α and strictly decreasing for $\mathcal{C}_{x_s}$.

We rewrite $\Xi(\alpha, \mathcal{C}_{x_s})$ as

$$\Xi(\alpha, \mathcal{C}_{x_s}) = \frac{(\gamma_s - 1)\xi}{\frac{\alpha}{1-\alpha}\left(1 + \sqrt{1 + (\gamma_s - 1)(1 - \mathcal{C}_{x_s}^2)}\right) + (\gamma_s - 1)\xi}. \tag{46}$$

The denominator of $\Xi(\alpha, \mathcal{C}_{x_s})$ is strictly increasing for α and strictly decreasing for $\mathcal{C}_{x_s}$, while the numerator does not change. Therefore, $\Xi(\alpha, \mathcal{C}_{x_s})$ is strictly decreasing for α and strictly increasing for $\mathcal{C}_{x_s}$.

We provide the following lemma to use the strictly monotonic property.

Lemma 3: Let $f_i(x)$ and $f_d(x)$ are strictly increasing and decreasing continuous functions for $x \in [x_{\min}, x_{\max}]$, respectively. Then $x^* = \arg\min_{x \in [x_{\min}, x_{\max}]} \max(f_i(x), f_d(x))$ can be obtained as follows:

Case 1) If $f_i(x_{\min}) \geq f_d(x_{\min})$, then $x^* = x_{\min}$.

Case 2) If $f_i(x_{\max}) \leq f_d(x_{\max})$, then $x^* = x_{\max}$.

Case 3) Otherwise, there exists a unique x_0 satisfying $f_i(x_0) = f_d(x_0)$ and $x^* = x_0$.

Proof: In the proof, we only consider $x \in [x_{\min}, x_{\max}]$ unless stated. Due to the monotonicity, $\min f_i(x) = f_i(x_{\min})$ and $\max f_d(x) = f_i(x_{\min})$. For Case 1, it can be seen that $\max(f_i(x), f_d(x)) = f_i(x)$ since $\min f_i(x) > \max f_d(x)$, resulting in $x^* = \arg\min f_i(x) = x_{\min}$.

For Case 2, it can be similarly proved.

For Case 3, the inequalities $f_i(x_{\min}) < f_d(x_{\min})$ and $f_i(x_{\max}) > f_d(x_{\max})$ are satisfied. In this case, x_0 satisfying $f_i(x_0) = f_d(x_0)$ always exists due to the intermediate value theorem and it is unique according to the strictly monotonic property [40]. From Case 2, we obtain $x_0 = \arg\min_{x \in [x_{\min}, x_0]} \max(f_i(x), f_d(x))$. Similarly, $x_0 = \arg\min_{x \in [x_0, x_{\max}]} \max(f_i(x), f_d(x))$. Therefore, $x_0 = \arg\min \max(f_i(x), f_d(x))$, which proves $x^* = x_0$. ■

We obtain x^* for Case 3 with bisection search according to the strictly monotonic property, which is much faster than grid search [40].

By using the asymptotic outage probabilities of WU and SU in (32) and (34), respectively, we reformulate the fairness maximization problem as

$$\begin{aligned} &\min_{\alpha, \mathcal{C}_{x_s}} \max\left(\frac{1}{\lambda_w} g_w^0,\ \Xi\right) \\ &\text{subject to} : 0 \leq \mathcal{C}_{x_s} \leq 1, \\ &\qquad 0 \leq \alpha \leq \min\left(\frac{1}{\sqrt{1 + (\gamma_w - 1)(1 - \mathcal{C}_{x_s}^2)}}, 0.5\right). \end{aligned} \tag{47}$$

We use the primal decomposition method to find the solution to the problem (47). For the fixed circularity coefficient $\mathcal{C}_{x_s}$, we formulate the master problem as

$$\begin{aligned} &\min_{\alpha} \max\left(\frac{1}{\lambda_w} g_w^0,\ \Xi\right) \\ &\text{subject to} : 0 \leq \alpha \leq \min\left(\frac{1}{\sqrt{1 + (\gamma_w - 1)(1 - \mathcal{C}_{x_s}^2)}}, 0.5\right). \end{aligned} \tag{48}$$

Note that

$$\frac{1}{\lambda_w} g_w^0(0, \mathcal{C}_{x_s}) = \frac{-1 + \sqrt{\gamma_w}}{P\lambda_w} \tag{49}$$

and $\Xi(0, \mathcal{C}_{x_s}) = 1$. Because the asymptotic analysis is valid for a large transmit power, we ignore the case of $\frac{-1+\sqrt{\gamma_w}}{P\lambda_w} \geq 1$. Therefore, the inequality $g_w^0(0, \mathcal{C}_{x_s})/\lambda_w < \Xi(0, \mathcal{C}_{x_s})$ always holds, which implies that Case 1 in Lemma 3 does not occur. Let $\alpha_{\max} = \frac{1}{\sqrt{1 + (\gamma_w - 1)(1 - \mathcal{C}_{x_s}^2)}}$, then $g_w^0(\alpha, \mathcal{C}_{x_s}) \to \infty$ as $\alpha \to \alpha_{\max}$. Therefore, if $\alpha_{\max} \leq 0.5$, i.e., $(\gamma_w - 1)(1 - \mathcal{C}_{x_s}^2) \geq 3$, Case 2 does not occur. Then, we can consider the following two cases.

Case 1) $(\gamma_w - 1)(1 - \mathcal{C}_{x_s}^2) < 3$ and $g_w^0(0.5, \mathcal{C}_{x_s})/\lambda_w \leq \Xi(0.5, \mathcal{C}_{x_s})$: This is Case 2 in Lemma 3. Therefore, $\alpha^* = 0.5$, i.e., the optimal point.

Algorithm 3 Suboptimal Solution Based on Asymptotic Analysis

Initialize
  Set a convergence parameter $\epsilon > 0$ as a small positive number.
  Set α and $\mathcal{C}_{x_s}$ satisfying the constraint of the problem (43).
  Set $p^* = \max\left(\frac{1}{\lambda_w} g_w^0,\ \Xi\right)$.
repeat
  if $(\gamma_w - 1)(1 - \mathcal{C}_{x_s}^2) < 3$ and $g_w^0(0.5, \mathcal{C}_{x_s})/\lambda_w < \Xi(0.5, \mathcal{C}_{x_s})$ **then**
    $\alpha = 0.5$.
  else
    Find α satisfying $g_w^0(\alpha, \mathcal{C}_{x_s})/\lambda_w = \Xi(\alpha, \mathcal{C}_{x_s})$ by using bisection search.
  end if
  if $\alpha^2\gamma_w < 1$ and $g_w^0(\alpha, 0)/\lambda_w < \Xi(\alpha, 0)$ **then**
    $\mathcal{C}_{x_s} = 0$
  else if $g_w^0(\alpha, 1)/\lambda_w > \Xi(\alpha, 1)$ **then**
    $\mathcal{C}_{x_s} = 1$
  else
    Find $\mathcal{C}_{x_s}$ satisfying $g_w^0(\alpha, \mathcal{C}_{x_s})/\lambda_w = \Xi(\alpha, \mathcal{C}_{x_s})$ by using bisection search.
  end if
  Set $p^*_{\text{prev}} = p^*$.
  Set $p^* = \max\left(\frac{1}{\lambda_w} g_w^0,\ \Xi\right)$.
until $p^*_{\text{prev}} - p^* < \epsilon$

Case 2) Otherwise: This is Case 3 in Lemma 3. Therefore, α^* satisfying $g_w^0(\alpha^*, \mathcal{C}_{x_s})/\lambda_w = \Xi(\alpha^*, \mathcal{C}_{x_s})$ is the optimal point.

For the fixed power allocation factor α, we formulate the subproblem as

$$\min_{\mathcal{C}_{x_s}} \max\left(\frac{1}{\lambda_w} g_w^0,\ \Xi\right)$$
$$\text{subject to}: \max\left(0, \frac{\alpha^2\gamma_w - 1}{\alpha^2(\gamma_w - 1)}\right) \le \mathcal{C}_{x_s} \le 1. \quad (50)$$

Let $\mathcal{C}_{\min} = \frac{\alpha^2\gamma_w - 1}{\alpha^2(\gamma_w - 1)}$, then $g_w^0(\alpha, \mathcal{C}_{x_s}) \to \infty$ as $\mathcal{C}_{x_s} \to \mathcal{C}_{\min}$. Therefore, if $\mathcal{C}_{\min} \ge 0$, i.e., $\alpha^2\gamma_w \ge 1$, Case 1 in Lemma 3 does not occur. Then, we can consider the following three cases.

Case 1) $\alpha^2\gamma_w < 1$ and $g_w^0(\alpha, 0)/\lambda_w \le \Xi(\alpha, 0)$: This is Case 1 in Lemma 3. Therefore, $\mathcal{C}^* = 0$, i.e., the optimal point.

Case 2) $g_w^0(\alpha, 1)/\lambda_w \ge \Xi(\alpha, 1)$: This is Case 2 in Lemma 3. Therefore, $\mathcal{C}^* = 1$, i.e., the optimal point.

Case 3) Otherwise: This is Case 3 in Lemma 3. Therefore, $\mathcal{C}^*$ satisfying $g_w^0(\alpha, \mathcal{C}^*)/\lambda_w = \Xi(\alpha, \mathcal{C}^*)$ is the optimal point.

By solving the master problem and the subproblem iteratively, which is depicted in Algorithm 3, we can obtain the suboptimal solution to the problem (43). Since bisection search is much faster than grid search, the computational complexity of Algorithm 3 is much lower than that of Algorithm 1 and Algorithm 2.

TABLE 1. Parameters used in simulation.

Parameter	Value
Channel variance of WU (λ_w)	1
Channel variance of SU (λ_s)	100
Level of residual interference (ξ)	0.001
Power allocation factor (α)	0.2
Target rate of WU ($R_{t,w}$)	2 bps/Hz
Target rate of SU ($R_{t,s}$)	4 bps/Hz

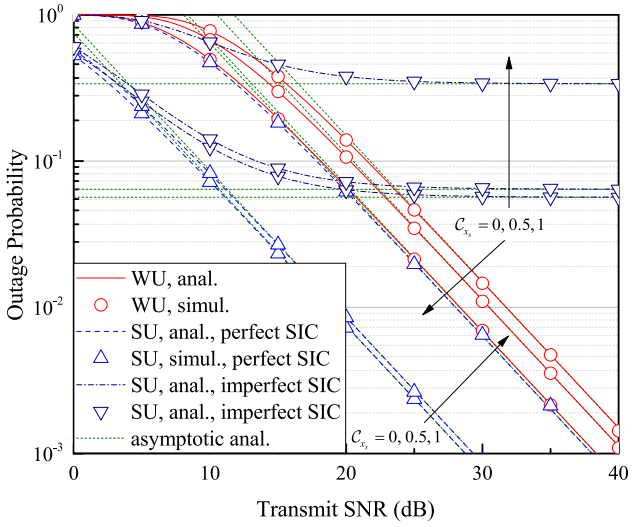

(a) $R_{t,s} = 4$ bps/Hz.

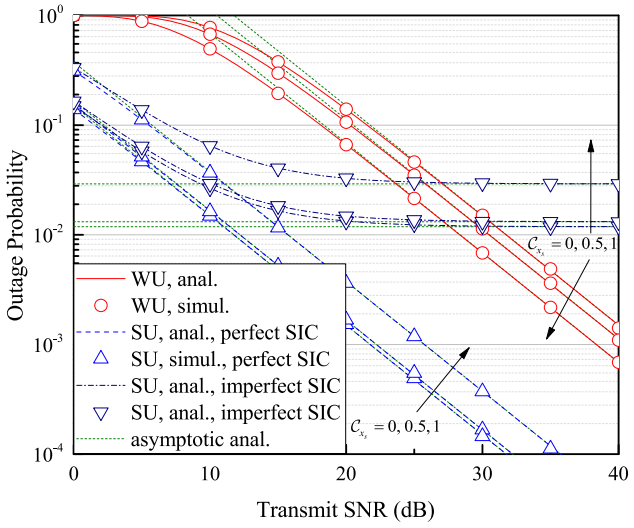

(b) $R_{t,s} = 2$ bps/Hz.

FIGURE 2. Outage probabilities of WU and SU.

V. SIMULATION RESULTS

For simulation, we use MATLAB with the Monte Carlo method. Unless specified, simulation parameters are set according to Table 1.

Fig. 2 show the outage probabilities of WU and SU according to the transmit SNR of the BS for SU's target rate of (a)

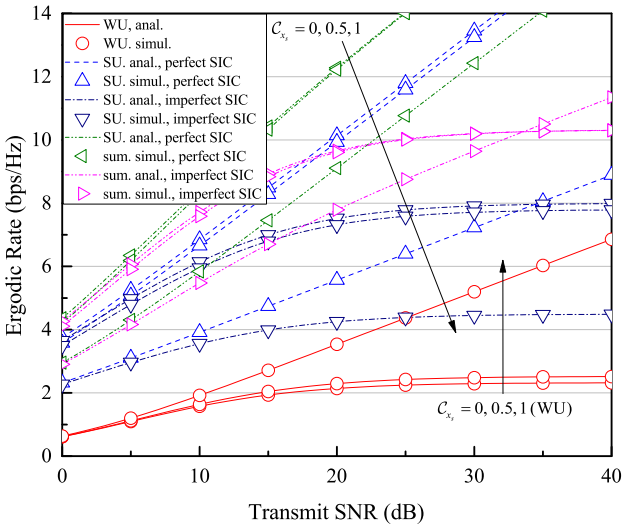

FIGURE 3. Ergodic rates of WU and SU, and their sum rates.

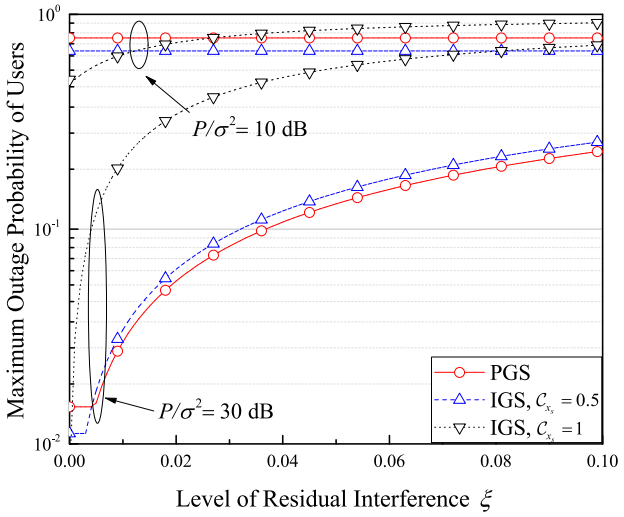

FIGURE 4. Maximum outage probability of each user versus level of residual interference.

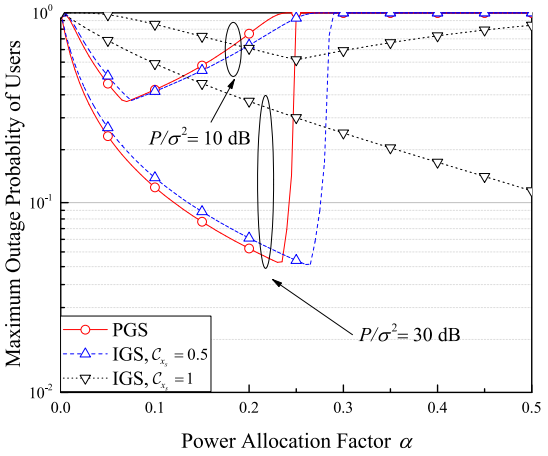

FIGURE 5. Maximum outage probability of each user versus power allocation factor.

4 bps/Hz and (b) 2 bps/Hz. In the figure, $\mathcal{C}_{x_s} = 0$ indicates that SU uses PGS. It shows that the outage probabilities of the two users decrease with the transmit SNR. It also shows that with the circularity coefficient, the outage probability of WU decreases while that of SU increases, for the perfect and imperfect SIC cases. When $\mathcal{C}_{x_s}$ is increased from 0 to 0.5, the outage probability of SU is slightly increased for both $R_{t,s} = 4$ bps/Hz and $R_{t,s} = 2$ bps/Hz, while that of WU is decreased further. On the other hand, when $\mathcal{C}_{x_s}$ is increased from 0.5 to 1, the outage probability of SU increased significantly, especially for $R_{t,s} = 4$, while that of WU is decreased little. From this, we can infer that by setting circularly coefficient appropriately, overall performance of the NOMA system can be improved. In the high SNR region, the outage probabilities converge to the asymptotic lines, and the error floor appears for SU with imperfect SIC.

Fig. 3 shows the ergodic rates of WU and SU, and their sum rates according to the transmit SNR of the BS. It shows that the ergodic rates of the both users and their sum rates increase with the transmit SNR. It also shows that with the circularity coefficient, the ergodic rate of WU increases while that of SU decreases, for the perfect and imperfect SIC cases. For the perfect SIC case, the sum rate decreases with the circularity coefficient. For the imperfect SIC case, with the circularity coefficient, the sum rate decreases in the low SNR region, but increases in the high SNR region.

Figs. 2 and 3 show that the analytical results perfectly match the simulation results, which verifies that our analysis is accurate. In the following figures, we only plot the analytical results for convenience.

Fig. 4 shows the maximum outage probability of each of the two users, i.e., $\max(p_w^{\text{out}}, p_s^{\text{out}})$, according to the level of residual interference. The low value of the maximum outage probability indicates that it achieves higher fairness of the NOMA system. It shows that for the transmit SNR of 10 dB, a maximally improper signal, i.e., $\mathcal{C}_{x_s} = 1$, achieves the lowest maximum outage probability, i.e., highest fairness, when the level of residual interference is low, while an improper signal with $\mathcal{C}_{x_s} = 0.5$ achieves the highest fairness when the level of residual interference is high. On the other hand, for the transmit SNR of 30 dB, a proper signal achieves highest fairness except when the level of residual interference is low. This indicates that the impropriety of a signal achieving the highest fairness depends on system parameters.

Fig. 5 shows the maximum outage probability of each user according to the power allocation factor. It shows that when the power allocation factor is high, the outage probabilities become one for a proper signal and an improper signal with $\mathcal{C}_{x_s} = 0.5$. This is an expected result according to Lemma 1 as the both users always experience outage when decoding WU's signal due to the interference from SU's signal.

On the other hand, a maximally improper signal does not make the outage probability one for any power allocation factor. This comes from the characteristics of IGS such that

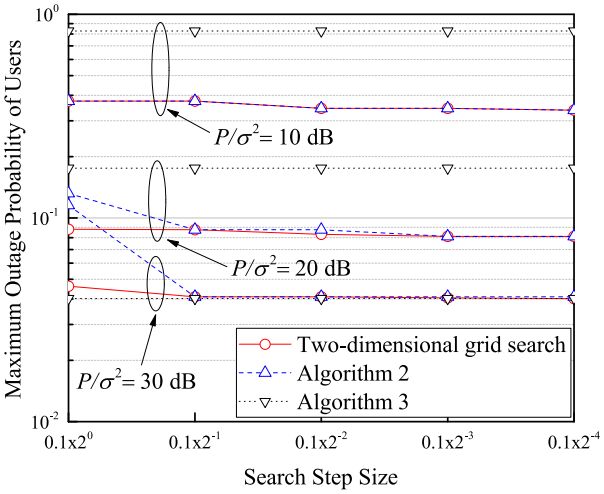

(a) Maximum outage probability of each user versus search step size.

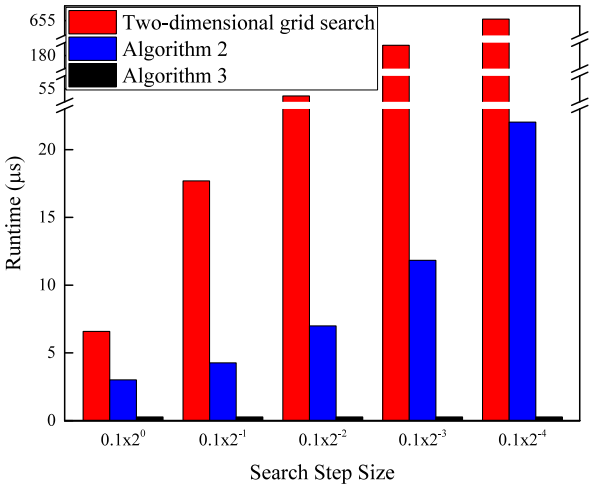

(b) Average runtime versus search step size with transmit SNR P/σ^2 = 20 dB. The CPU used in the simulation is Intel Core i7-3770.

FIGURE 6. Performance comparison between two-dimensional grid search and the proposed algorithms.

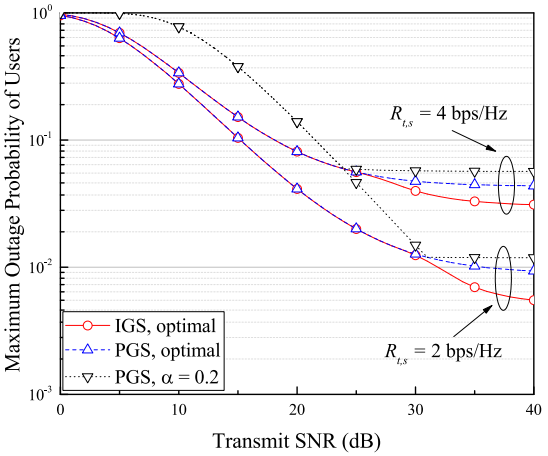

FIGURE 7. Maximum outage probability of each user versus transmit SNR.

it reduces the effects of interference. It also shows that a proper signal achieves the highest fairness when the power allocation factor is low, while a maximally proper signal achieves the highest fairness when the power allocation factor is high. For the transmit SNR of 10 dB, a proper signal achieves the maximum fairness, while for the transmit SNR of 30 dB, an improper signal with $\mathcal{C}_{x_s} = 0.5$ achieves the maximum fairness. This indicates that IGS has an advantage in the high SNR region. This is the expected result due to the characteristics of IGS. Since IGS improves performance in the interference channel, not the AWGN channel, it is natural that IGS shows better performance in the high SNR region.

Fig. 6 shows performance comparison between two-dimensional grid search and the proposed algorithms according to the search step size. Algorithm 3 uses bisection search of which accuracy and computational complexity do not depend on the search step size. Therefore, the performance of Algorithm 3 does not change with the search step size. Fig. 6 (a) shows that two-dimensional grid search with a very small step size, for example $\varepsilon = 0.1x2^4$, achieves the optimal point. It shows that the accuracy of two-dimensional grid search and Algorithm 2 increase as the search step size decreases. It also shows that Algorithm 2 achieves almost the same accuracy with two-dimensional grid search.

For the transmit SNR of 10 dB and 20 dB, the accuracy of Algorithm 3 is very poor but converges to that of two-dimensional grid search as the transmit SNR increases. This is because Algorithm 3 uses the asymptotic results which are valid in the high SNR region. In Fig. 6 (b), Algorithm 3 shows great performance compared to the other methods in terms of runtime. As the search step size increases, runtime in the two-dimensional grid search increases dramatically, which is too high compared to that in the proposed algorithms.

Fig. 7 shows the maximum outage probability of each user according to the transmit SNR. For the case of PGS, we optimize only the power allocation factor, and for the case of IGS, we optimize both the power allocation factor and the impropriety of the signal. For the accurate results, we use two dimensional grid search with search step size $\varepsilon = 0.001$. It shows that fairness is improved by solving the optimization problem for the both PGS and IGS cases. In the low SNR region, the maximum outage probability is the same for the PGS and IGS cases with optimization. However, in the high SNR region, it shows that IGS achieves higher fairness compared to PGS. From this, we can see that IGS is effective for the case when transmit SNR is high. It also shows that IGS can improve the fairness of the NOMA system for SU's target rate of both 4 bps/Hz and 2 bps/Hz cases.

Fig. 8 shows the sum rate of each user according to the level of residual interference. It shows that the sum rate decreases according to the level of residual interference. It also shows that a proper signal and an improper signal with $\mathcal{C}_{x_s} = 0.5$ obtain almost the same sum rate. For the transmit SNR of 10 dB, a maximally improper signal lowers the sum rate. For the transmit SNR of 30 dB, a maximally improper signal lowers the sum rate when the level of residual interference is low, while it improves the sum rate when the level of residual interference is high.

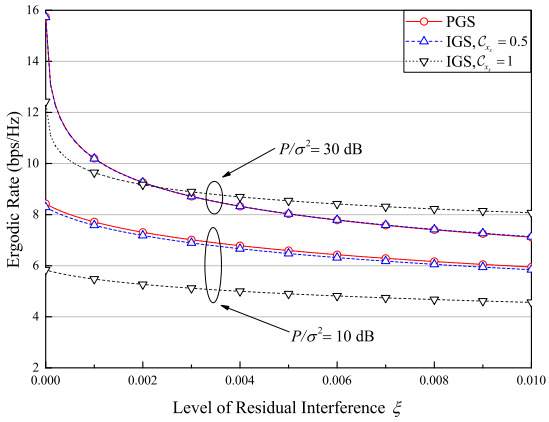

FIGURE 8. Sum rate of each user versus level of residual interference.

VI. CONCLUSION

In this paper, we investigated a NOMA system consisting of a BS and two users. A user whose channel condition has been significantly degraded due to path loss and shadowing effects is called WU and the other user is called SU. We applied IGS and PGS to SU and WU, respectively, and derived the outage probabilities and the ergodic rates of the both users in the closed form, assuming imperfect SIC. Due to imperfect SIC, the diversity order of WU decreases from one to zero. We proposed two algorithms to maximize the fairness of the NOMA system. We confirmed that the simulation results match the analytical results very well. We showed that WU exploits an advantage of using IGS at the expense of SU's performance, i.e., achieving improved fairness of the NOMA system. We also showed that using the proposed algorithms, we obtain the optimal solution that maximizes fairness with low computational complexity, especially in the high SNR region. In future work, we will also apply IGS to WU, extend the system model to a cellular network that supports more users and design an improper signal modulation scheme suitable for NOMA systems.

APPENDIXES

APPENDIX A

PROOF OF LEMMA 1

If Eq. (12) does not hold, i.e., $\alpha \geq 1/\sqrt{1+(\gamma_w-1)(1-\mathcal{C}_{x_s}^2)}$, the second and first order coefficients of g_w in the quadratic function inside the probability in (11) satisfy the following inequalities:

$$\begin{aligned} A &= P^2(1-\alpha^2\gamma_w+\alpha^2\gamma_w\mathcal{C}_{x_s}^2-\alpha^2\mathcal{C}_{x_s}^2) \\ &= P^2(1-\alpha^2(1+(\gamma_w-1)(1-\mathcal{C}_{x_s}^2))) \\ &\leq 0 \end{aligned} \tag{51}$$

and

$$\begin{aligned} B &= 2P(1-\alpha\gamma_w) \\ &\leq 2P\left(1-\frac{\gamma_w}{\sqrt{\gamma_w-\mathcal{C}_{x_s}^2(\gamma_w-1)}}\right) \\ &\overset{(a)}{<} 2P(1-\sqrt{\gamma_w}) \\ &< 0 \end{aligned} \tag{52}$$

where $\gamma_w-\mathcal{C}_{x_s}^2(\gamma_w-1) < \gamma_w$ in (a) since $\gamma_w > 1$. We see that the value of the quadratic function is always negative for $g_w > 0$ since all the coefficients in the quadratic function are negative. This means that if Eq. (12) does not hold, the outage probability of WU always becomes one.

APPENDIX B

PROOF OF LEMMA 2

Let $h(g_r)$ be the quadratic function in g_r inside the probability on the RHS of Eq. (19), i.e.,

$$\begin{aligned} h(g_r) = {} & P^2(\gamma_s-1)(1-\alpha)^2g_r^2-2P(1-\alpha)(P\alpha g_s-(\gamma_s-1)) \\ & \times g_r-P^2\alpha^2(1-\mathcal{C}_{x_s}^2)g_s^2-2P\alpha g_s+(\gamma_s-1). \end{aligned} \tag{53}$$

The y-intercept of $h(g_r)$ is given by

$$y(g_s) = -P^2\alpha^2(1-\mathcal{C}_{x_s}^2)g_s^2-2P\alpha g_s+(\gamma_s-1). \tag{54}$$

The positive root of $h(g_r)$ is $g_r^0(g_s)$ if $y(g_s) > 0$, and that of $y(g_s)$ is g_s^0. It is easy to see that $y(g_s) > 0$ if g_s is smaller than the positive root of $y(g_s)$, and $y(g_s) < 0$ otherwise.

When $y(g_s) > 0$, i.e., $g_s \in (0, g_s^0)$, the symmetry axis of $h(g_r)$ becomes negative because

$$\frac{P\alpha g_s-(\gamma_s-1)}{P(\gamma_s-1)(1-\alpha)} = -\frac{y(g_s)+P^2\alpha^2(1-\mathcal{C}_{x_s}^2)g_s^2+P\alpha g_s}{P(\gamma_s-1)(1-\alpha)} < 0, \tag{55}$$

which makes $h(g_r) > 0$ regardless of g_r.

When $y(g_s) < 0$, i.e., $g_s \in (g_s^0, \infty)$, it is easy to see that $h(g_r) > 0$ if and only if g_r is larger than the positive root of $h(g_r)$, i.e., $g_r \in (g_r^0(g_s), \infty)$.

APPENDIX C

PROOF OF THEOREM 3

From (1), (7), and (35), we obtain the ergodic rate of WU as

$$\begin{aligned} \bar{R}_w &= \frac{1}{2}\int_0^\infty \log_2\left(\frac{(Pg+1)^2-(P\alpha g\mathcal{C}_{x_s})^2}{(P\alpha g+1)^2-(P\alpha g\mathcal{C}_{x_s})^2}\right) f_{g_w}(g)dg \\ &= \frac{1}{2\lambda_w}\Bigg(\underbrace{\int_0^\infty \log_2((Pg+1)^2-(P\alpha g\mathcal{C}_{x_s})^2)e^{-\frac{1}{\lambda_w}g}dg}_{=F} \\ &\quad -\int_0^\infty \log_2((P\alpha g+1)^2-(P\alpha g\mathcal{C}_{g_s})^2)e^{-\frac{1}{\lambda_w}g}dg\Bigg). \end{aligned} \tag{56}$$

We calculate the first integral term on the RHS of Eq. (56) as

$$\begin{aligned} F &= \int_0^\infty \log_2((Pg+1)^2-(P\alpha g\mathcal{C}_{x_s})^2)e^{-\frac{1}{\lambda_w}g}dg \\ &= -\lambda_w\log_2(P^2(1-\alpha^2\mathcal{C}_{x_s}^2)g^2+2Pg+1)e^{-\frac{1}{\lambda_w}g}\Big|_0^\infty \\ &\quad +\frac{2\lambda_w}{\ln 2}\int_0^\infty\left(\frac{P^2(1-\alpha^2\mathcal{C}_{x_s}^2)g+P}{P^2(1-\alpha^2\mathcal{C}_{x_s}^2)g^2+2Pg+1}\right)e^{-\frac{1}{\lambda_w}g}dg \\ &\overset{(b)}{=} -\frac{\lambda_w}{\ln 2}\left(e^{\frac{1}{P\lambda_w(1-\alpha\mathcal{C}_{x_s})}}\mathrm{Ei}\left(-\frac{1}{P\lambda_w(1-\alpha\mathcal{C}_{x_s})}\right)\right. \\ &\quad \left.+e^{\frac{1}{P\lambda_w(1+\alpha\mathcal{C}_{x_s})}}\mathrm{Ei}\left(-\frac{1}{P\lambda_w(1+\alpha\mathcal{C}_{x_s})}\right)\right) \end{aligned} \tag{57}$$

$$\begin{aligned}\bar{R}_s &= \frac{1}{2}\int_0^\infty\int_0^\infty \log_2\left(\frac{(P\alpha g + P(1-\alpha)\tilde{g}+1)^2 - (P\alpha g\mathcal{C}_{x_s})^2}{(P(1-\alpha)\tilde{g}+1)^2}\right) f_{g_s}(g)dg f_{g_r}(\tilde{g})d\tilde{g}\\ &= \frac{1}{2}\int_0^\infty\int_0^\infty \log_2\left((P\alpha g + P(1-\alpha)\tilde{g}+1)^2 - (P\alpha g\mathcal{C}_{x_s})^2\right)\frac{1}{\lambda_s}e^{-\frac{1}{\lambda_s}g}dg f_{g_r}(\tilde{g})d\tilde{g}\\ &\quad -\frac{1}{\xi\lambda_s}\int_0^\infty \log_2(P(1-\alpha)\tilde{g}+1)e^{-\frac{1}{\xi\lambda_s}\tilde{g}}d\tilde{g}\\ &\overset{(c)}{=} \frac{1}{2\xi\lambda_s\ln 2}\int_0^\infty\Bigg[\underbrace{-e^{\frac{P(1-\alpha)\tilde{g}+1}{P\alpha\lambda_s(1-\mathcal{C}_{x_s})}}\mathrm{Ei}\left(-\frac{P(1-\alpha)\tilde{g}+1}{P\alpha\lambda_s(1-\mathcal{C}_{x_s})}\right)}_{=G} - e^{\frac{P(1-\alpha)\tilde{g}+1}{P\alpha\lambda_s(1+\mathcal{C}_{x_s})}}\mathrm{Ei}\left(-\frac{P(1-\alpha)\tilde{g}+1}{P\alpha\lambda_s(1+\mathcal{C}_{x_s})}\right)\Bigg]e^{-\frac{1}{\xi\lambda_s}\tilde{g}}d\tilde{g}. \end{aligned} \tag{58}$$

$$\begin{aligned}\int_0^\infty Ge^{-\frac{1}{\xi\lambda_s}\tilde{g}}d\tilde{g} &= \int_0^\infty e^{\frac{P(1-\alpha)\tilde{g}+1}{P\alpha\lambda_s(1-\mathcal{C}_{x_s})}}\mathrm{Ei}\left(-\frac{P(1-\alpha)\tilde{g}+1}{P\alpha\lambda_s(1-\mathcal{C}_{x_s})}\right)e^{-\frac{1}{\xi\lambda_s}\tilde{g}}d\tilde{g}\\ &\overset{(d)}{=} \frac{\alpha\lambda_s(1-\mathcal{C}_{x_s})}{1-\alpha}e^{\frac{1}{P(1-\alpha)\xi\lambda_s}}\int_{\frac{1}{P\alpha\lambda_s(1-\mathcal{C}_{x_s})}}^\infty e^{\left(1-\frac{\alpha\lambda_s(1-\mathcal{C}_{x_s})}{(1-\alpha)\xi\lambda_s}\right)\tilde{h}}\mathrm{Ei}(-\tilde{h})d\tilde{h}\\ &\overset{(e)}{=} -\frac{\alpha\xi\lambda_s(1-\mathcal{C}_{x_s})}{(1-\alpha)\xi-\alpha(1-\mathcal{C}_{x_s})}e^{\frac{1}{P(1-\alpha)\xi\lambda_s}}\left[\mathrm{Ei}\left(-\frac{\alpha\lambda_s(1-\mathcal{C}_{x_s})}{(1-\alpha)\xi\lambda_s}\tilde{h}\right) - e^{\left(1-\frac{\alpha\lambda_s(1-\mathcal{C}_{x_s})}{(1-\alpha)\xi\lambda_s}\right)\tilde{h}}\mathrm{Ei}(-\tilde{h})\right]\Bigg|_{\frac{1}{P\alpha\lambda_s(1-\mathcal{C}_{x_s})}}^\infty\\ &= \frac{\alpha\xi\lambda_s(1-\mathcal{C}_{x_s})}{(1-\alpha)\xi-\alpha(1-\mathcal{C}_{x_s})}\left[e^{\frac{1}{P(1-\alpha)\xi\lambda_s}}\mathrm{Ei}\left(-\frac{1}{P(1-\alpha)\xi\lambda_s}\right) - e^{\frac{1}{P\alpha\lambda_s(1-\mathcal{C}_{x_s})}}\mathrm{Ei}\left(-\frac{1}{P\alpha\lambda_s(1-\mathcal{C}_{x_s})}\right)\right]. \end{aligned} \tag{59}$$

where (b) is derived by using the integral in [41]. Then we calculate the second integral term on the RHS of Eq. (56) in the similar way.

From (2), (9), and (36), we obtain the ergodic rate of SU in (58), as shown at the top of this page, where (c) is derived in the similar way used in (57). The first term in the integral on the RHS of Eq. (58) is derived in (59), as shown at the top of this page, where (d) is derived by putting $-\frac{P(1-\alpha)\tilde{g}+1}{P\alpha\lambda_s(1-\mathcal{C}_{x_s})}$ into $\tilde{h}$, and (e) is derived by using the integral in [42]. We calculate the other terms in the integral in the similar way. Then we finally obtain the ergodic rates of SU and WU, i.e., $\bar{R}_s$ and $\bar{R}_w$, as given above.

REFERENCES

[1] Y. Saito, Y. Kishiyama, A. Benjebbour, T. Nakamura, A. Li, and K. Higuchi, "Non-orthogonal multiple access (NOMA) for cellular future radio access," in *Proc. IEEE 77th Veh. Technol. Conf. (VTC Spring)*, Dresden, Germany, Jun. 2013, pp. 1–5.

[2] A. Benjebbour, Y. Saito, Y. Kishiyama, A. Li, A. Harada, and T. Nakamura, "Concept and practical considerations of non-orthogonal multiple access (NOMA) for future radio access," in *Proc. Int. Symp. Intell. Signal Process. Commun. Syst.*, Okinawa, Japan, Nov. 2013, pp. 770–774.

[3] Z. Ding, Z. Yang, P. Fan, and H. V. Poor, "On the performance of non-orthogonal multiple access in 5G systems with randomly deployed users," *IEEE Signal Process. Lett.*, vol. 21, no. 12, pp. 1501–1505, Dec. 2014.

[4] L. Dai, B. Wang, Y. Yuan, S. Han, C.-L. I, and Z. Wang, "Non-orthogonal multiple access for 5G: Solutions, challenges, opportunities, and future research trends," *IEEE Commun. Mag.*, vol. 53, no. 9, pp. 74–81, Sep. 2015.

[5] Z. Ding, Y. Liu, J. Choi, Q. Sun, M. Elkashlan, C.-L. I, and H. V. Poor, "Application of non-orthogonal multiple access in LTE and 5G networks," *IEEE Commun. Mag.*, vol. 55, no. 2, pp. 185–191, Feb. 2017.

[6] A. Goldsmith, *Wireless Communications*. Cambridge, U.K.: Cambridge Univ. Press, 2005.

[7] F. D. Neeser and J. L. Massey, "Proper complex random processes with applications to information theory," *IEEE Trans. Inf. Theory*, vol. 39, no. 4, pp. 1293–1302, Jul. 1993.

[8] P. J. Schreier and L. L. Scharf, *Statistical Signal Processing of Complex-Valued Data: The Theory of Improper and Noncircular Signals*. Cambridge, U.K.: Cambridge Univ. Press, 2010.

[9] Z. K. M. Ho and E. Jorswieck, "Improper Gaussian signaling on the two-user SISO interference channel," *IEEE Trans. Wireless Commun.*, vol. 11, no. 9, pp. 3194–3203, Sep. 2012.

[10] H. Park, S. H. Park, J. S. Kim, and I. Lee, "SINR balancing techniques in coordinated multi-cell downlink systems," *IEEE Trans. Wireless Commun.*, vol. 12, no. 2, pp. 626–635, Feb. 2013.

[11] Y. Zeng, C. M. Yetis, E. Gunawan, Y. L. Guan, and R. Zhang, "Transmit optimization with improper Gaussian signaling for interference channels," *IEEE Trans. Signal Process.*, vol. 61, no. 11, pp. 2899–2913, Jun. 2013.

[12] A. Napolitano and C. M. Spooner, "Cyclic spectral analysis of continuous-phase modulated signals," *IEEE Trans. Signal Process.*, vol. 49, no. 1, pp. 30–44, Jan. 2001.

[13] H. D. Nguyen, R. Zhang, and S. Sun, "Improper signaling for symbol error rate minimization in K-user interference channel," *IEEE Trans. Commun.*, vol. 63, no. 3, pp. 857–869, Mar. 2015.

[14] E. Kurniawan and S. Sun, "Improper Gaussian signaling scheme for the Z-interference channel," *IEEE Trans. Wireless Commun.*, vol. 14, no. 7, pp. 3912–3923, Jul. 2015.

[15] C. Lameiro, I. Santamaria, and P. J. Schreier, "Rate region boundary of the SISO Z-interference channel with improper signaling," *IEEE Trans. Commun.*, vol. 65, no. 3, pp. 1022–1034, Mar. 2017.

[16] C. Hellings and W. Utschick, "Improper signaling versus time-sharing in the SISO Z-interference channel," *IEEE Commun. Lett.*, vol. 21, no. 11, pp. 2432–2435, Nov. 2017.

[17] C. Lameiro, I. Santamaría, and P. J. Schreier, "Benefits of improper signaling for underlay cognitive radio," *IEEE Wireless Commun. Lett.*, vol. 4, no. 1, pp. 22–25, Feb. 2015.

[18] C. Lameiro, I. Santamaria, and P. J. Schreier, "Improper Gaussian signaling for multiple-access channels in underlay cognitive radio," *IEEE Trans. Commun.*, vol. 67, no. 3, pp. 1817–1830, Mar. 2019.

[19] M. Gaafar, O. Amin, A. Ikhlef, A. Chaaban, and M.-S. Alouini, "On alternate relaying with improper Gaussian signaling," *IEEE Commun. Lett.*, vol. 20, no. 8, pp. 1683–1686, Aug. 2016.

[20] M. Gaafar, M. G. Khafagy, O. Amin, R. F. Schaefer, and M.-S. Alouini, "Full-duplex relaying with improper Gaussian signaling over Nakagami-m fading channels," *IEEE Trans. Commun.*, vol. 66, no. 1, pp. 64–78, Jan. 2018.

[21] I. Abu Mahady, E. Bedeer, S. Ikki, and H. Yanikomeroglu, "Sum-rate maximization of NOMA systems under imperfect successive interference cancellation," *IEEE Commun. Lett.*, vol. 23, no. 3, pp. 474–477, Mar. 2019.
[22] H. D. Tuan, A. A. Nasir, H. H. Nguyen, T. Q. Duong, and H. V. Poor, "Non-orthogonal multiple access with improper Gaussian signaling," *IEEE J. Sel. Topics Signal Process.*, vol. 13, no. 3, pp. 496–507, Jun. 2019.
[23] D. Tse and P. Viswanath, *Fundamentals of Wireless Communication*. Cambridge, U.K.: Cambridge Univ. Press, 2005.
[24] X. Chen, R. Jia, and D. W. K. Ng, "On the design of massive non-orthogonal multiple access with imperfect successive interference cancellation," *IEEE Trans. Commun.*, vol. 67, no. 3, pp. 2539–2551, Mar. 2019.
[25] M. F. Kader, M. B. Shahab, and S. Y. Shin, "Exploiting non-orthogonal multiple access in cooperative relay sharing," *IEEE Commun. Lett.*, vol. 21, no. 5, pp. 1159–1162, May 2017.
[26] G. Im and J. H. Lee, "Outage probability for cooperative NOMA systems with imperfect SIC in cognitive radio networks," *IEEE Commun. Lett.*, vol. 23, no. 4, pp. 692–695, Apr. 2019.
[27] F. Cui, Z. Qin, Y. Cai, M. Zhao, and G. Y. Li, "Rethinking outage constraints for resource management in NOMA networks," *IEEE J. Sel. Topics Signal Process.*, vol. 13, no. 3, pp. 423–435, Jun. 2019.
[28] X. Yue, Y. Liu, S. Kang, A. Nallanathan, and Y. Chen, "Modeling and analysis of two-way relay non-orthogonal multiple access systems," *IEEE Trans. Commun.*, vol. 66, no. 9, pp. 3784–3796, Sep. 2018.
[29] X. Yue, Z. Qin, Y. Liu, S. Kang, and Y. Chen, "A unified framework for non-orthogonal multiple access," *IEEE Trans. Commun.*, vol. 66, no. 11, pp. 5346–5359, Nov. 2018.
[30] C. Yan, A. Harada, A. Benjebbour, Y. Lan, A. Li, and H. Jiang, "Receiver design for downlink non-orthogonal multiple access (NOMA)," in *Proc. IEEE 81st Veh. Technol. Conf. (VTC Spring)*, Glasgow, Scotland, May 2015, pp. 1–6.
[31] K. Saito, A. Benjebbour, Y. Kishiyama, Y. Okumura, and T. Nakamura, "Performance and design of SIC receiver for downlink NOMA with open-loop SU-MIMO," in *Proc. IEEE Int. Conf. Commun. Workshop (ICCW)*, London, U.K., Jun. 2015, pp. 1161–1165.
[32] L. Bariah, S. Muhaidat, and A. Al-Dweik, "Error probability analysis of non-orthogonal multiple access over Nakagami-*m* fading channels," *IEEE Trans. Commun.*, vol. 67, no. 2, pp. 1586–1599, Feb. 2019.
[33] Q. He, Y. Hu, and A. Schmeink, "Closed-form symbol error rate expressions for non-orthogonal multiple access systems," *IEEE Trans. Veh. Technol.*, vol. 68, no. 7, pp. 6775–6789, Jul. 2019.
[34] S. Li, M. Derakhshani, and S. Lambotharan, "Outage-constrained robust power allocation for downlink MC-NOMA with imperfect SIC," in *Proc. IEEE Int. Conf. Commun. (ICC)*, Kansas City, MO, USA, May 2018, pp. 1–7.
[35] M. M. Abramowitz and I. A. Stegun, *Handbook of Mathematical Functions: With Formulas, Graphs, and Mathematical Tables*, 10th ed. New York, NY, USA: Dover, 1972.
[36] S. M. R. Islam, N. Avazov, O. A. Dobre, and K.-S. Kwak, "Power-domain non-orthogonal multiple access (NOMA) in 5G systems: Potentials and challenges," *IEEE Commun. Surveys Tuts.*, vol. 19, no. 2, pp. 721–742, 2nd Quart., 2017.
[37] D. P. Palomar and M. Chiang, "A tutorial on decomposition methods for network utility maximization," *IEEE J. Sel. Areas Commun.*, vol. 24, no. 8, pp. 1439–1451, Aug. 2006.
[38] W. Wu, X. Yin, P. Deng, T. Guo, and B. Wang, "Transceiver design for downlink SWIPT NOMA systems with cooperative full-duplex relaying," *IEEE Access*, vol. 7, pp. 33464–33472, 2019.
[39] W. Wu, F. Zhou, R. Q. Hu, and B. Wang, "Energy-efficient resource allocation for secure NOMA-enabled mobile edge computing networks," *IEEE Trans. Commun.*, vol. 68, no. 1, pp. 493–505, Jan. 2020.
[40] R. L. Burden, J. D. Faires, and A. M. Burden, *Numerical Analysis*, 10th ed. Boston, MA, USA: Brooks/Cole, 2015.
[41] A. P. Prudnikov, Y. A. Brychkov, and O. I. Marichev, *Integrals and Series: Elementary Functions*, vol. 1. New York, NY, USA: Gordon and Breach, 1986.
[42] A. P. Prudnikov, Y. A. Brychkov, and O. I. Marichev, *Integrals and Series: Special Functions*, vol. 2. New York, NY, USA: Gordon and Breach, 1986.

SEUNG GEUN HONG received the B.S. degree in electrical engineering and the Ph.D. degree in electrical engineering and computer science from Seoul National University (SNU), Seoul, South Korea, in 2013 and 2020, respectively. He is currently a Staff Engineer with Samsung Electronics, Suwon, South Korea. His research activities are in physical layer wireless communications, such as NOMA systems, D2D communication, and mmWave networks.

SAEWOONG BAHK (Senior Member, IEEE) received the B.S. and M.S. degrees in electrical engineering from Seoul National University (SNU), in 1984 and 1986, respectively, and the Ph.D. degree from the University of Pennsylvania, in 1991. He was a member of Technical Staff with AT&T Bell Laboratories, from 1991 to 1994, where he had worked on network management. From 2009 to 2011, he served as the Director of the Institute of New Media and Communications. He is currently a Professor with SNU. He has been leading many industrial projects on 3G/4G/5G and the IoT connectivity supported by Korean industry. He has published more than 200 technical articles and holds more than 100 patents. He is a member of the National Academy of Engineering of Korea (NAEK) and of Whos Who Professional in Science and Engineering. He was a recipient of the KICS Haedong Scholar Award, in 2012. He was the General Chair of the IEEE DySPAN 2018 (Dynamic Spectrum Access and Networks) and the Director of the Asia-Pacific Region of the IEEE ComSoc. He was the TPC Chair of the IEEE VTC-Spring 2014, the General Chair of JCCI 2015, the Co-Editor-in-Chief of *Journal of Communications and Networks* (JCN), and on the Editorial Board of *Computer Networks* (COMNET) journal and the IEEE TRANSACTIONS ON WIRELESS COMMUNICATIONS (TWireless). He has been serving as the Chief Information Officer (CIO) of SNU and the General Chair of the IEEE WCNC 2020 (Wireless Communication and Networking Conference). He is the President of the Korean Institute of Communications and Information Sciences (KICS). He is an Editor of the *IEEE Network Magazine*.